Quantification and Mapping of Tissue Damage from Freezing in Cod by Magnetic Resonance Imaging

Kathryn E. Anderssen [a]*, Shaheen Syed [a,b], Svein Kristian Stormo [a]

* Corresponding author. E-mail: kate.anderssen@nofima.no

[a] Department of Seafood Industry, Nofima AS, P.O. Box 6122, 9291 Tromsø, Norway

[b] Department of Computer Science, UiT The Arctic University of Norway, Tromsø, Norway

Abstract

Freezing of fish is an important processing method that can extend the shelf life of the product but can also lead to significant damage to the tissue if performed incorrectly. In order to thoroughly evaluate different freezing protocols, a method to characterize the extent and distribution of damage from freezing is needed. Magnetic resonance imaging (MRI) was tested as a technique to map and quantify tissue damage from freezing in fish. Groups of packaged cod (*Gadus morhua)* loin were frozen to either -5, -20, or -40 °C, thawed and then imaged with a T_2-weighted MRI sequence. Areas of damage appear as bright clusters in the muscle tissue. To provide repeatable, objective classification, image analysis using a convolutional neural network was then performed on the MRI data to identify regions of damaged tissue. As expected, the colder the freezing procedure, the less damage the process generally produced. Results show non-uniform damage throughout the fillet, with tissue damage due to freezing concentrated in the center of the fillet. This suggests that surface limited methods, such as hyperspectral imaging, may not fully capture the extent of damage due to freezing and thawing. The percent of tissue classified as damaged by the neural network generally correlated well with liquid loss (*cor* = 0.83).

Keywords: magnetic resonance imaging; fish; cod; freezing; image analysis; deep learning

1 INTRODUCTION

Freezing of fish is commonly used to extend the shelf life of a product and ensure year-round availability of seasonable products (Johnston et al., 1994). However, the freezing procedure used may greatly impact the ultimate product quality. Research has shown that fish that has been frozen slowly is of lower quality upon thawing than fish that has been frozen quickly (Love 1956; Chen and Pan, 1997; Johnston et al., 1994). A low freezing rate may lead to more liquid loss upon thawing and subsequent cold storage and is often associated with undesirable sensory properties like dryness, toughness, and chewiness (MacCallums 1966; Hurling 1996). The reason for this is physical damage of the tissue from ice crystals, which tear the cellular structure. The low freezing-rate allows larger ice crystals to form, which in turn causes larger amounts of damage (Petzold and Aguilera 2009; van der Sman et al. 2013; Dalvi-Isfahan et al., 2019). While some producers use blast freezing to freeze their fish, many still rely on slow freezing where the fish is placed in still air. Despite its widespread use, recent studies indicate that this method of freezing may not be sufficient to avoid significant tissue damage from freezing (Washburn et al. 2017). Furthermore, advanced methods for freezing have been developed, such as ultrasound assisted freezing (Delgado and Sun, 2011) or brine freezing. While not technically a freezing method, superchilling causes a significant fraction of the water in the fish to be frozen (Duun and Rustad, 2007). The effect of these treatments on product quality has not been fully explored. As such, the ability to quantify damage to tissue would be a valuable research tool to better understand and improve the freezing process in order to produce the highest quality products.

A variety of methods have been used to evaluate damage caused by freezing in fish. Measurement of liquid loss is one of the most commonly used techniques (Ofstad et al., 1996). Here, the percent of liquid lost by the sample is correlated with tissue damage. Texture measurements have also been used to evaluate freezing damage, as the cellular breakdown from the ice crystals results in a softer texture (Mørkøre and Lilleholt 2007; Saez et al. 2015; Nakazawa and Okazaki 2020). Other studies have used microscopy to investigate what happens on a cellular level (Sigurgisladottir et al., 2000). Shrinking of

51 the myofibrils and an increase in the extracellular space in the muscle structure is evident. However,
52 all these methods have the drawback in that they lack spatial resolution. Tissue damage to the fish will
53 not be uniform. Fillets will freeze unevenly, the surface freezing quickly while the center of the fish
54 takes longer. Because the tissue damage is tied to freezing rate, it is expected that the amount of
55 damage will vary throughout the sample. Therefore, a technique that can both map and quantify
56 damage to tissue would be ideal. Hyperspectral imaging has been used to characterize damage from
57 freezing (Washburn et al., 2017; Xu and Sun, 2017), but it is limited in that, at best, it can only measure
58 the top centimeter of a sample.

59 In this study, we used magnetic resonance imaging (MRI) as an alternative method to quantify
60 damage to tissue. This technique has been used previously to image the effect of salting on cod
61 (Erikson et al. 2004; Gudjónsdóttir et al. 2015) and salmon (Aursand et al. 2009; Veliyulin et al. 2007).
62 MRI uses a strong magnetic field, radio frequency pulses and magnetic gradients to create an image of
63 a sample (Callaghan 1993). In most situations, MRI is used to measure the amount of hydrogen
64 throughout the sample. In biological samples, as hydrogen is predominantly located in constituents
65 like water and fat, MRI produces an image of the soft tissue. While MRI can be used to provide an
66 absolute quantification of the hydrogen present, measurements can also be performed to produce
67 contrast between different types of features in the image. One way to produce contrast in MRI images
68 is transverse relaxation, or T_2 relaxation. This property describes how quickly the MRI signal decays
69 away. In general, the MRI signal associated with tightly bound hydrogen, such as hydrogen in proteins,
70 relaxes very quickly. In contrast, hydrogen in free diffusing liquids has a longer transverse relaxation
71 rate. T_2-weighting is an MRI method that can be used to highlight the presence of damage in the muscle
72 structure. Previous research on meat and fish has shown that freezing and thawing will damage tissue,
73 such that the transverse relaxation time becomes longer (Lambelet et al. 1995; Jensen et al. 2002;
74 Mortensen et al 2006; Bertram et al 2007; Sánchez-Alonso et al. 2012; Sánchez-Alonso et al. 2014,
75 Duflot et al. 2019). This is believed to be due to tissue damage causing less restriction of the water
76 molecules. Therefore, by identifying regions of longer T_2 relaxation, tissue damage can be identified.

During T_2-weighted MRI imaging, the measurement is performed in a manner that causes regions of different T_2 values to have different contrast in the image. The signal from regions with shorter T_2 relaxation will decay away more quickly, so they will appear darker in the image. Similarly, the signal regions with longer T_2 relaxation times decay away more slowly and they will appear brighter in the image. In medical research, this approach has been used to identify a variety of different damages and disease in the brain (Welch et al. 1995; Shibata et al. 2000) and heart (Abdel-Aty et al. 2007).

Although prior studies have used MRI to image frozen and thawed fish products (Howell et al. 1996; Nott et al. 1999), improvements to MRI microimaging equipment in recent years allows much higher resolution images to be produced, making detailed image analysis possible. In this study, T_2-weighted MRI images were used to characterize cod tissue before and after different freezing protocols. While qualitative inspection of the MRI images for damage is useful, quantification of the amount and location of tissue damage would provide valuable information for researchers studying the effect of different types of processing protocols. A challenge, however, is accurate segmentation of tissue into damaged and non-damaged regions. In some situations, it is straight forward to identify areas of damaged and non-damaged tissue. Frequently though, the damage in tissue is often scattered throughout the sample and the precise change between damaged and not damaged areas is not obvious, making its identification manually both arduous and subjective. There is likely to be significant variation depending on who performs the classification. To overcome this problem, image analysis is then applied using a convolutional neural network to quantify and map the distribution of damage throughout the sample. This allows a rapid, repeatable way to classify the tissue in MRI images into damaged and non-damaged regions.

2 MATERIALS AND METHODS

2.1 MRI PROCEDURES

MRI images were taken using a 7 Tesla MR Solutions (United Kingdom) small animal imager using the large rat quadrature coil. Images were taken in the axial direction using the Fast Spin Echo T_2-weighted sequence. Repetition time (TR) was 8 seconds, slice thickness was 1mm and the number of slices was 54. Field of View was 60mm and each image was 256 x 256 pixels, giving a resolution of approximately 240 microns. Images were stored in 12 bit grayscale values.

2.2 NMR PROCEDURES

Transverse relaxation measurements were made using a 43 Mhz Magritek SpinSolve (Aachen, Germany) system. Small samples of tissue were placed in 5mm tubes for measurement. Transverse relaxation was measured using the standard Carr-Purcell-Meiboom-Gill sequence (Carr and Purcell, 1954; Meiboom and Gill, 1958). Pulse length was 12.5 μs, echo spacing was 80 μs and TR was 5 seconds. Inversion of the data was performed using a Butler-Reed-Dawson algorithm (Butler et al. 1981) built into the spectrometer operating software.

2.3 SAMPLES

Sixteen Atlantic cod fish (*Gadus morhua*) were provided by Tromsø Aquaculture Research Station, Norway. The fish were killed by a blow to the head and immediately gutted. They were bled for 30 mins, iced and transported to Nofima, where they were kept on ice for 4 days to ensure that the fish were out of rigor prior to filleting. The fillets were then sliced into loin pieces (n=32, 146g ± 19g) and vacuum packed (99%) in plastic pouches (20 μm polyamide inside layer and 70 μm polyethylene outside layer, O_2 permeability: 45 $cm^3/(m^2\ d\ bar)^{-1}$). In order to create consistent samples, sections were taken from the same location in the loin of all the fillets. Packed samples were stored on ice until imaging in the MRI scanner. After imaging, the samples were then split into groups of three. Group 1

(n=11) was frozen to -5 °C. It is well established that freezing at this high of temperature will produce a highly damaged sample (Mørkøre and Lilleholt, 2007). At -5 °C, large ice crystals can form and a significant fraction of water will remain in an unfrozen state (Powrie 1984). This leads to melting and recrystallisation in the tissue, increasing cellular damage (Braslavsky 2015). This freezing protocol was used to provide an end point of what extremely damaged tissue looks like. Realistically, it is not expected this situation would occur often, perhaps arising if there were some fault with the freezing equipment or if fillets are bulk stacked before freezing (Johnston 1994). Group 2 (n=11) was frozen in still air to -20 °C. This is most similar to the typical freezing procedure present in industrial settings. Group 3 (n=10) was blast frozen to -40 °C (3 ms^{-1}), which previous studies has shown causes less damage to fish tissue (Mørkøre and Lilleholt, 2007; Anderssen et al. 2020). All samples were frozen, stored for 5 days, then thawed rapidly in a 4 °C circulating water bath for two hours. Samples were kept in the vacuum bags to avoid direct contact between the water and fillets. After thawing, samples were stored on ice until imaging in the MRI scanner and subsequent liquid loss measurements were performed following imaging.

2.4 LIQUID LOSS

Liquid loss was collected directly from the vacuum packages. The vacuum-packed samples containing fish muscle and expelled liquid were opened after MRI imaging before and after freezing and frozen storage. Liquid loss (LL, %) was determined according to the formula:

$$LL = \frac{m_0 - m_L}{m_0} \times 100\ \%$$

where m_0 is the initial weight of the loin, and m_L is the weight of the loin after packaging, MRI imaging, frozen storage and final MRI imaging.

2.5 IMAGE ANALYSIS

2.5.1 PREPROCESSING

MRI images were read from the DICOM (.dcm) file format with the python library pydicom (v1.4.2) and stored in hierarchical data format 5 (HDF5) for further analyses. Image artifacts due to the plastic wrapping surrounding the cod loins were removed by segmenting each image slice into 2 distinct classes, the background and the foreground (i.e., the cod loin). To do this, images were converted to 8 bits, and a max filter, erosion, and Gaussian blur were applied. These steps increased the distinction between the background and foreground. Next, the k-means clustering algorithm was applied to segment the image into two distinct classes. A mask of the background class was then used to set each background pixel to the value zero.

To enable a supervised machine learning process of tissue classification, tissue was manually annotated into regions of: (i) damaged tissue, (ii) non-damaged tissue, (iii) damaged connective tissue (i.e., myocommata), and (iv) non-damaged connective tissue. Annotations were created using the tool ITK-SNAP (Yushkevich et al., 2006). Afterwards, regions of annotated tissue were converted into 8 x 8 pixels features by employing a sliding window approach over the regions with a step size of 1, and the class labels representing one of the four regions. A total of 545,882 damaged, 2,415,618 non-damaged, 15,315 damaged connective tissue, and 53,956 non-damaged connective tissue features were created. Features from the minority classes were randomly oversampled so as to create a class balanced dataset.

2.5.2 CONVOLUTIONAL NEURAL NETWORK

A convolutional neural network (CNN) was trained to classify the features into the four classes. The proposed CNN architecture was inspired by the VGG16 architecture (Simonyan and Zisserman, 2015),

which was one of the winning entries of 2014 edition of the ImageNet Large Scale Visual Recognition Challenge (Russakovsky et al., 2015). Details about the architecture can be found in Table S1 in the supplementary material. The proposed architecture contained a total of 8 million trainable parameters.

Training was performed on 80% of the feature data, with 10% data for validation and 10% for testing the CNN model on new unseen data. The model was trained for a total of 100 epochs with stochastic gradient descent, a learning rate of 0.05, and a batch size of 32 images. Two types of regularization techniques were used to prevent the CNN model from overfitting to the training data. Firstly, early stopping was implemented, essentially terminating training if the validation loss did not increase for 20 epochs. When early stopping terminated the learning process, the model with the best weights with respect to the validation loss was restored. Secondly, the CNN model used several dropout layers (Srivastava et al., 2014), which has shown to significantly improve the performance of the neural network in several domains. The proposed CNN model achieved an accuracy of 0.976 on the training set, 0.952 on the validation set, and 0.952 on the test set after early stopping terminated the learning process at 50 epochs. Training results per epoch can be found in Figure S1 in the supplementary material. Furthermore, the CNN model was constructed using the Python library TensorFlow 2.1.0 (Abadi et al., 2016) and trained on two Nvidia RTX-2080Ti and one Nvidia Titan RTX graphical processing units.

2.5.3 POST-PROCESSING

Each image (i.e., a single MRI slice) was then classified into regions of damage, non-damage, damaged connective tissue, and non-damaged connective tissue. A sliding window approach (Harzallah et al., 2009; Szegedy et al., 2013) with a stride of 4 pixels was utilized to classify regions of 8 x 8 pixels with the trained CNN classification model, focusing only on the tissue and ignoring the background. Regions

of connective tissue were additionally ignored and only regions of damaged and non-damaged were considered in the analysis. Select images are shown in this paper and the complete set of images with classified regions are available upon reasonable request.

3 RESULTS

3.1 LIQUID LOSS

The liquid loss results are in line with previous research, showing that lower freezing temperatures were correlated with lower liquid loss, Figure 1.

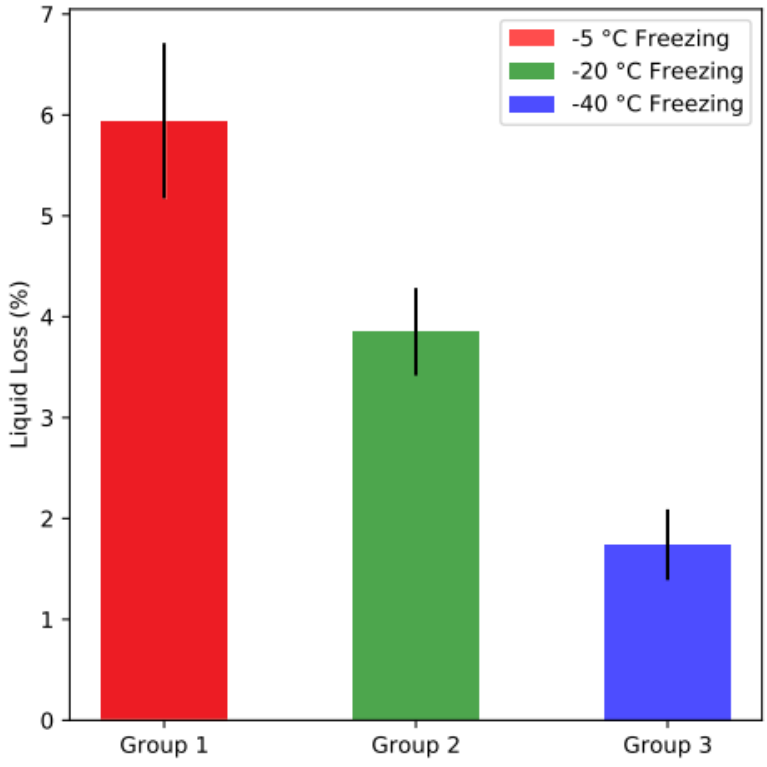

Figure 1: Liquid loss results for the three different groups of freezing procedures. The error bars show the standard error of the mean.

The average liquid loss for Group 1 was 6.0% with a standard deviation of 1.2%. Group 2 had a liquid loss of 3.9% with a standard deviation of 0.7% and Group 3 had a liquid loss of 1.7% with a standard

deviation of 0.5%. ANOVA analysis of the data shows statistically significant differences between the groups ($F(2,30)=68.82$, p = 9.74e-12).

3.2 The effect of Freezing Procedure on T_2 Distribution

Figure 2 shows an example of the changes in the T_2 times of a frozen and thawed cod sample depending on freezing procedure used.

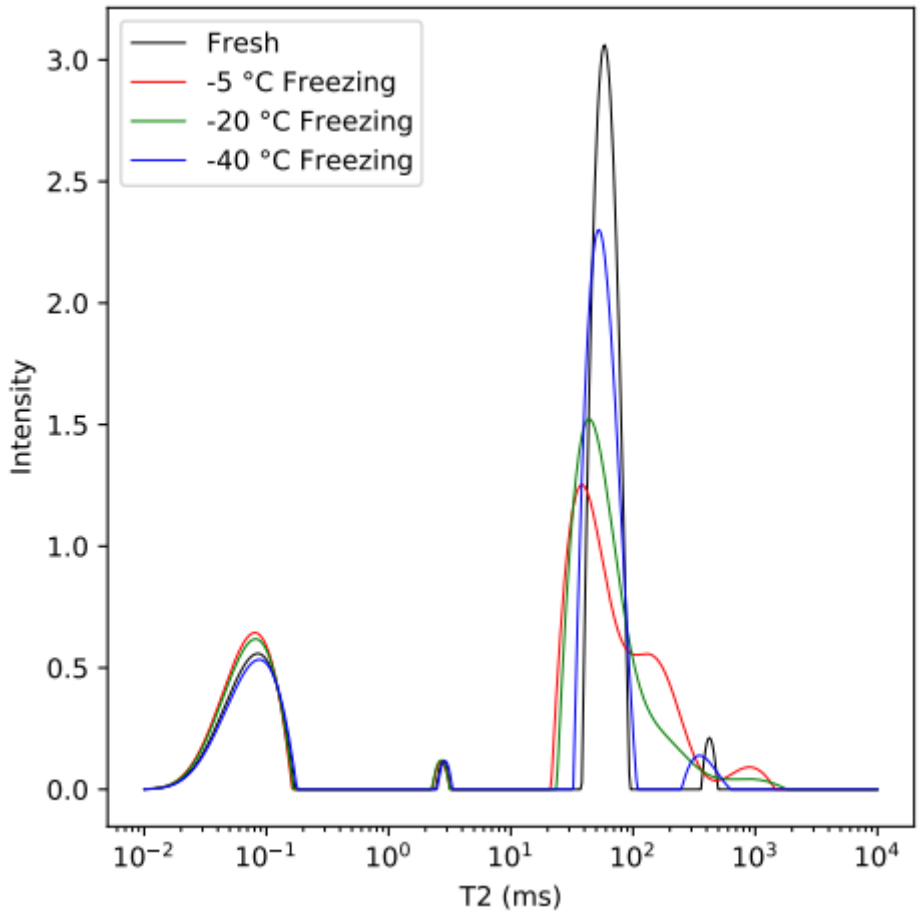

Figure 2: T_2 distributions of fresh cod tissue and tissue that has been frozen at -5, -20 and -40 °C and subsequently thawed

There are 4 peaks in the T_2 distribution of cod muscle. The shortest peak around 0.1 ms is associated with hydrogen in the tissue itself. The peak at 2-3 ms is hydrogen in water tightly associated with macromolecules. The main peak (approx. 50 ms) arises from water within the myofibrillar matrix. The longest relaxing peak (approx. 300 ms) is water in extra-myofibrillar spaces (Bertram et al. 2001). When tissue is damaged, water is lost from the myofibrillar matrix and is able to leak into the extra-

myofibrillar regions, leading to a decrease in the main peak and an increase in longer T_2 values (Mortensen et al. 2007). The sample frozen to -40°C shows a very similar distribution of T_2 times as the fresh state, with only some minor broadening of the main peak and extra-myofibrillar peak. The sample frozen to -20 °C shows a shift to longer T_2 times. The sample frozen to -5 °C shows a significant shift. These data agree with results found by previous researchers. Therefore, when MRI imaging is performed with T_2-weighting, as regions with tissue damage have longer T_2 values, they will appear brighter in the image.

3.3 IMAGE CLASSIFICATION

Figure 3 shows an example of an axial image of a fillet from Group 1 before and after freezing to -5 °C and the respective classification of tissue performed by the image analysis.

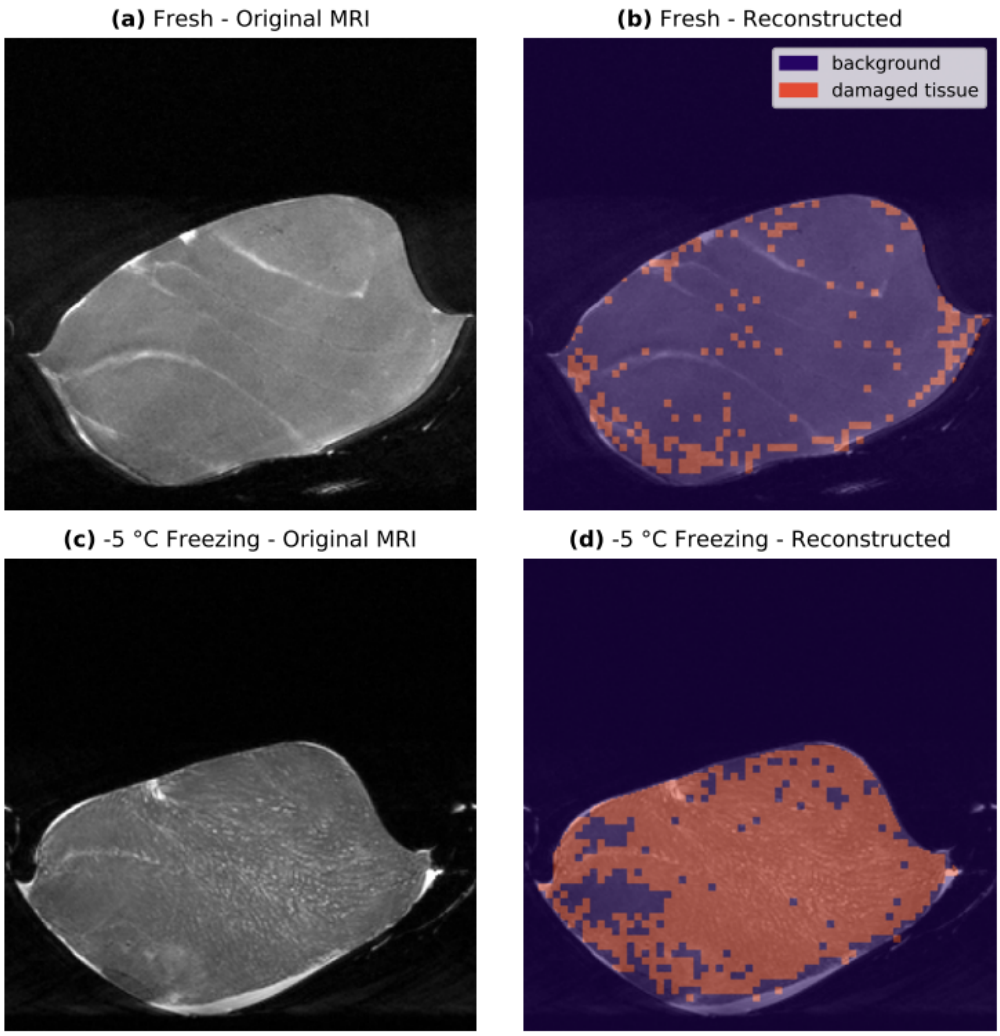

Figure 3: Example of a) Original MRI image of a sample in the fresh state b) image of sample in the fresh state with damaged tissue identified c) Original MRI image of a sample that has been frozen to -5°C and thawed d) Image of sample that has been frozen to -5°C and thawed with damaged tissue identified

While the original fillets were overall in good condition, a small amount of tissue is classified as damaged in the fresh state for Group 1 (mean= 11.5%, std=5.1%). This is to be expected, as some tissue damage will occur due to handling and the filleting process. However, after freezing and thawing, nearly all the tissue in the sample is classified damaged (mean= 81.2%, std=14.3%). Note, due to minor differences in sample orientation and changes in the tissue during freezing, there will not be perfect alignment between the images of the samples in the fresh and thawed state. While there seems to be slightly less damage on the edges of the samples, overall the extent of the tissue damage is so great that almost the entirety of the sample can be considered damaged. The bright edges surrounding the sample are liquid loss trapped in the vacuum pack.

Figure 4 shows an example axial image from Group 2 before and after freezing to -20 ˚C and the respective classification of tissue performed by the image analysis.

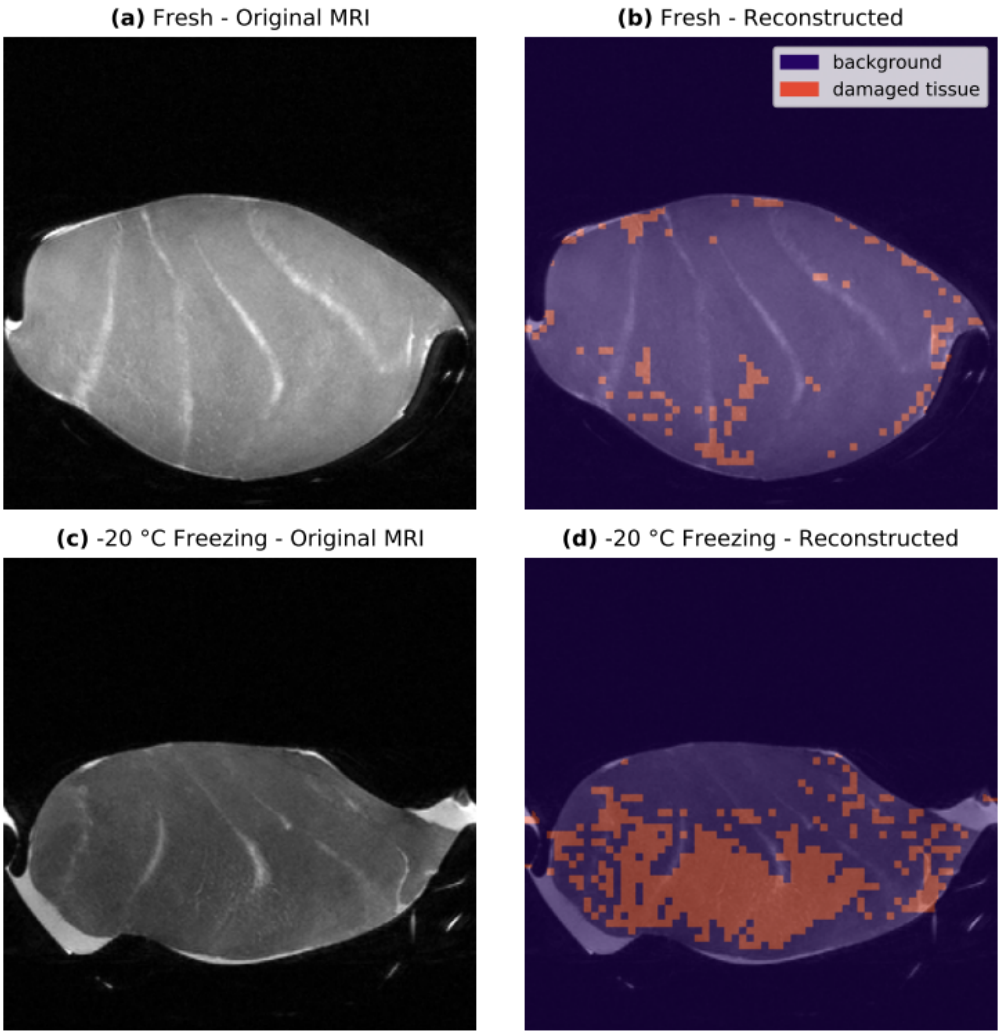

Figure 4: Example of a) Original MRI image of a sample in the fresh state b) image of sample in the fresh state with damaged tissue identified c) Original MRI image of a sample that has been frozen to -20°C and thawed d) Image of sample that has been frozen to -20°C and thawed with damaged tissue identified

As with Group 1, Group 2 showed minor damage in the fresh state (mean=8.3%, std=2.8%). After freezing, there was a noticeable increase in tissue classified as damaged (mean=57.4%, std=13.3%). Although damage could be found throughout the fillet, frequently the damage was localized towards the center of the fillet. This is in line with freezing theory, where the surface of the sample will freeze more quickly while the center takes longer and is therefore more prone to damage. As with samples in Group 1, prominent liquid loss surrounding the samples could often be seen in Group 2.

Figure 5 shows an example axial image from Group 3 before and after freezing to -40 ˚C and the respective classification of tissue performed by the image analysis.

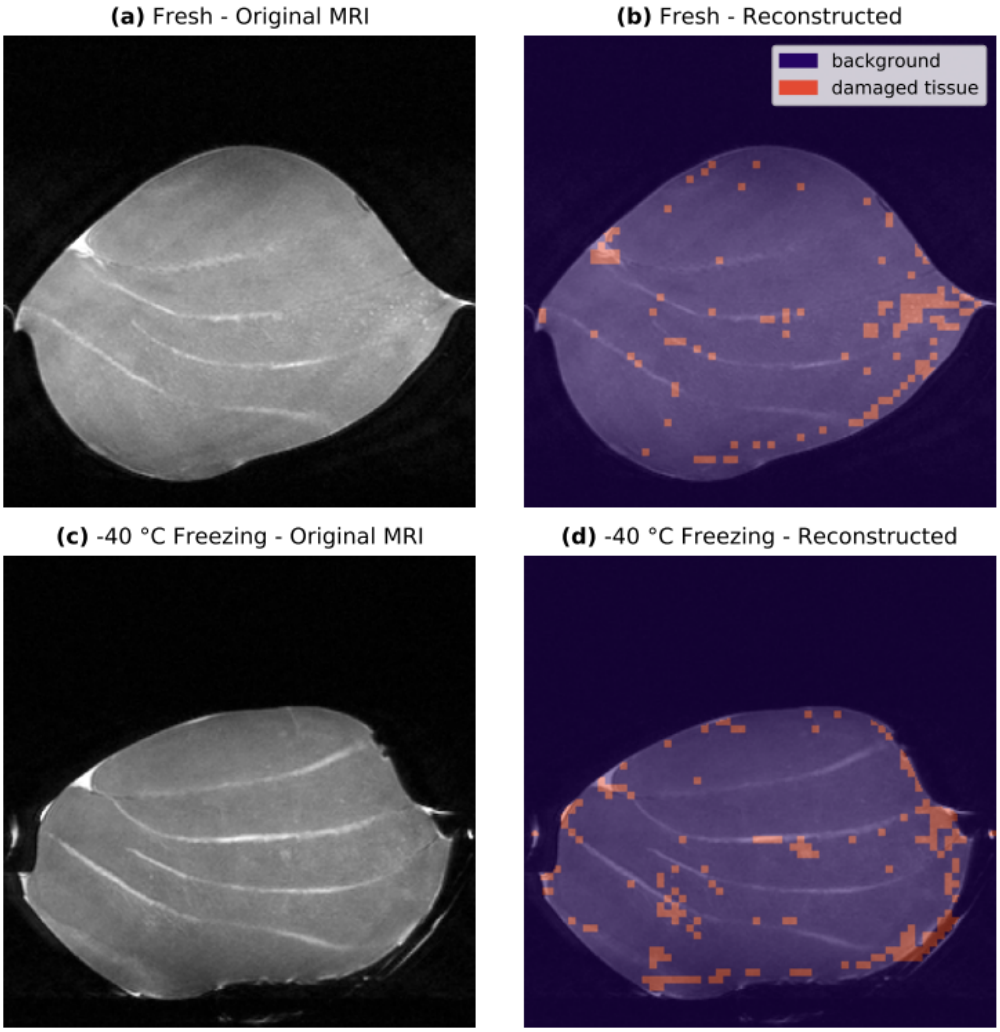

Figure 5: Example of a) Original MRI image of a sample in the fresh state b) image of sample in the fresh state with damaged tissue identified c) Original MRI image of a sample that has been frozen to -40°C and thawed d) Image of sample that has been frozen to -40°C and thawed with damaged tissue identified

Minor tissue damage was observed in the fresh state (mean= 8.9%, std=3.5%). Only a minor increase in was observed in the thawed state (mean = 15.9%, std=5.4%). No particular localization of tissue damage was noted in the -40°C samples. Only minor liquid loss was observed around the samples.

3.4 Statistical Analysis of Results

In order to aid comparison of results, a histogram of the damaged tissue for the different groups is shown in Figure 6. The histogram shows the distribution for each group of the percentage of tissue classified as damaged for each of the axial slices for all the samples.

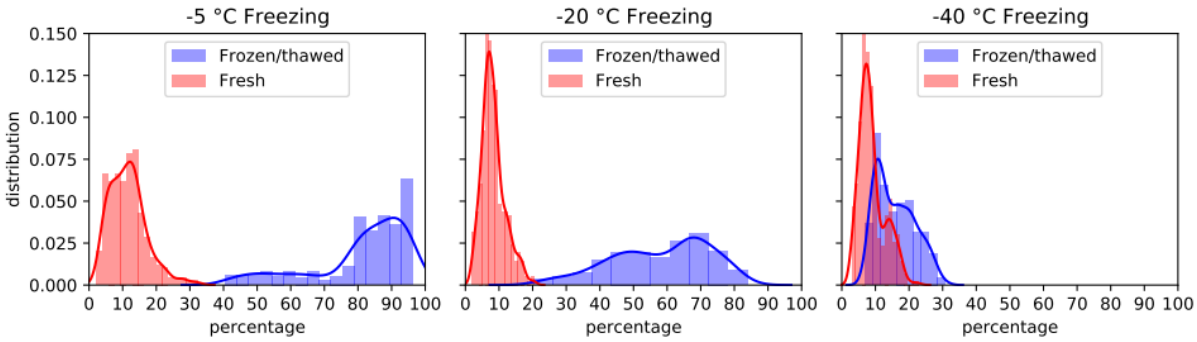

Figure 6: Histograms of the percent of tissue classified as damaged for each MRI image in both the fresh and then thawed state for the three different freezing protocols

All the groups showed minor damage in the fresh state. ANOVA analysis of the classified tissue in the fresh state did not show statistically significant differences in amounts of damaged tissue between the groups ($F(2,30)=2.11$, $p=0.14$). In contrast, ANOVA analysis of the classified tissue in the thawed state showed large statistically significant difference in the amount of damaged tissue between the groups ($F(2,30)=80.14$, $p=1.53e-12$). The percent damaged tissue versus liquid loss is plotted in Figure 7.

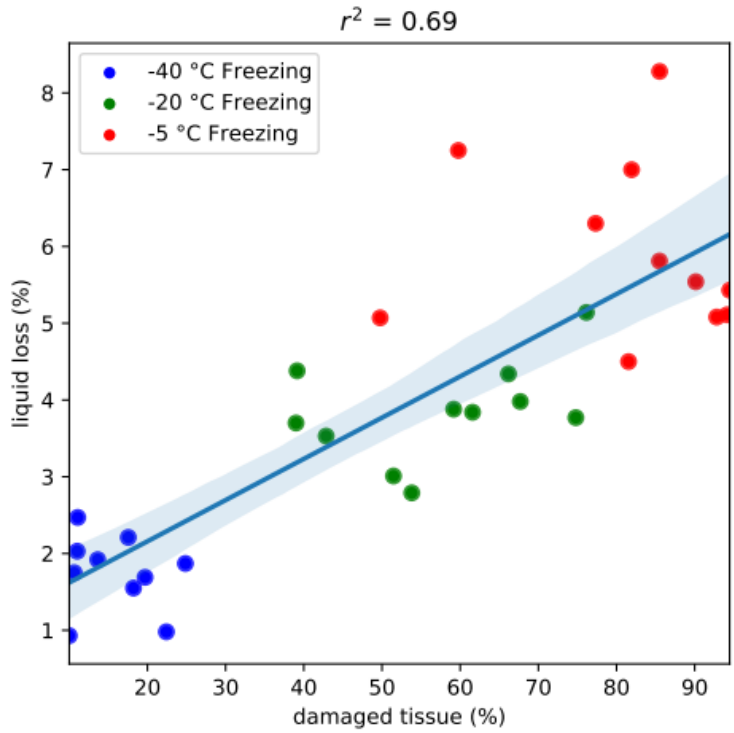

Figure 7: Plot of the relationship between the average amount of tissue classified as damaged in the MRI image and the sample liquid loss

There is a generally linear relationship between the two, with an r^2 of 0.69. The Pearson's correlation coefficient between liquid loss and damaged tissue is 0.83.

4 DISCUSSION

The results indicate that MRI is a promising method to identify tissue damage in fish, from both freezing and thawing and other sources. Classification of the images using a convolutional neural network appears to be an efficient approach to perform objective, repeatable identification of tissue damage in the MRI images. Although training the neural network is a slow process, once trained, it can classify future images in a matter of seconds. This makes it particularly valuable when numerous samples will be used. For the T_2-weighted images, tissue damage appears as clusters of bright spots in the image. This indicates that when tissue is damaged, liquid leaks from the myofibrillar structure and creates small pools in between the muscle fibers. We noted that in many cases, the connective tissue

appeared bright white in the images. Typically, the connective tissue appears darker than the surrounding muscle. This is due to a shorter T_2 value caused by the more rigid structure of the connective tissue and potentially the accumulation of fat. The images suggest that water collects in the connective tissue between the myomeres and that it serves as a conduit for liquid loss out of the sample. For the thawed samples in Groups 1 and 2, the overall intensity of the muscle tissue tended to decrease compared to the fresh state. We attribute this to liquid escaping from the myofibrillar matrix into pools between the muscle fibers, into the connective tissue and into the vacuum bag outside the sample.

Samples frozen to -20 °C incurred significantly more damage than samples frozen to -40 °C, suggesting the quality of frozen fish available to the consumer could be improved by increasing the freezing rate. For the -20°C samples, damage frequently concentrated towards the center of the loins. This agrees with freezing theory, as the center of the sample will freeze more slowly than the surface and, as such, would be expected to experience more damage. These results have several implications. First, surface techniques like near-infrared or hyperspectral imaging may not penetrate deep enough into the sample to adequately assess the full extent of damage to a sample. Secondly, it suggests that for analyses that use a small subsection of the sample, multiple subsections are necessary in order to avoid drawing a conclusion about the entire sample that may only be correct for a localized portion of it.

While the results are very promising for using MRI and image analysis to automatically classify damaged tissue in fish, the current study had several limitations. A challenge with the T_2-weighted images is that the brightness in the image is a function of both the water content and the local T_2 relaxation time. Future work aims to overcome this limitation by a performing a complete T_2 mapping of the sample. This will enable quantification of both the fluid content and T_2 time for each pixel, allowing an even more detailed description of tissue changes. The obstacle with this approach is that measurement time for each sample will be significantly longer, introducing concerns of sample stability during the course of the measurement program.

Another drawback of the study is that it performs a very black and white classification of the tissue, lumping all damaged tissue into one category. In reality, there is a range of severity of tissue damage. This is reflected in the relationship between the percent of tissue classified as damaged and liquid loss. While the current correlation is good, it is expected that a full T_2 mapping of the sample would improve the correlation between liquid loss and identified tissue damage. Another limitation with the chosen analysis method is that it relies on human input for training the classification of damaged and non-damaged tissue. While some signs of damage to the tissue are easy to spot visually, it is likely that there may be other indications of tissue damage that are less obvious. Further study is underway testing unsupervised classification to better identify all the features that are indicative of damage to tissue. Testing is planned to measure additional physical and chemical properties as well as measuring attributes such as sensory properties in order to attempt to relate them to MRI images.

5 CONCLUSIONS

Magnetic resonance imaging is a promising method for mapping and quantifying damage in fish products. Image analysis of the data using a trained neural network enables rapid classification of the tissue in the MRI images into damaged and non-damaged regions in an objective, repeatable manner. Classified tissue results correlated well with traditional liquid loss measurements. Results of the study indicate that blast freezing to -40 °C produces much less damage to the tissue than the industry standard of -18°C, emphasizing the need to change industry protocols if quality is to be improved. The damage in some of the fresh state samples highlights the need for thorough characterization of samples before undertaking a study to avoid unrelated effects from influencing results. The non-uniform damage indicates that surface methods like hyperspectral imaging may underestimate damage from freezing.

6 ACKNOWLEDGEMENTS

This project is supported by NFR funding grant 294805 and is a part of Nofima's Strategic Research Project (SIS) "FRESK", funded by Research Council of Norway (Institute Core Funding). This research is also part of Spectec, a Norwegian Strategic Research Initiative. The authors thank the PET-Senter at the Universitetssykhuset Nord-Norge for access to the MRI scanner.

7 REFERENCES

Abadi, M., Barham, P., Chen, J., Chen, Z., Davis, A., Dean, J., Devin, M., Ghemawat, S., Irving, G., Isard, M., Kudlur, M., Levenberg, J., Monga, R., Moore, S., Murray, D. G., Steiner, B., Tucker, P., Vasudevan, V., Warden, P., … Zheng, X. (2016). TensorFlow: A system for large-scale machine learning. 12th USENIX Symposium on Operating Systems Design and Implementation (OSDI 16), 265–283., doi: 10.5555/3026877.3026899

Abdel-Aty, H., Simonetti, O., Friedrich, M.G. (2007) T2-weighted cardiovascular magnetic resonance imaging, J. Magn Reson Imag, 26(3), 452-459, doi: 10.1002/jmri.21028

Anderssen, K.E., Stormo, S.K., Skåra, T., Skjelvareid, M.H., Heia, K. Predicting liquid loss of frozen and thawed cod from hyperspectral imaging, LWT, 133, 110093, doi: 10.1016/j.lwt.2020.110093

Aursand, I.G., Veliyulin, E., Bocker, U., Ofstad, R., Rustad, T., Erikson, U., (2009). Water and Salt Distribution in Atlantic Salmon (Salmo salar) Studied by Low-Field 1H NMR, 1H and 23Na MRI and Light Microscopy: Effects of Raw Material Quality and Brine Salting., J. Agric. Food Chem, 57(1): 46-54, doi: 10.1021/jf802158u

Bertram, H.C., Karlsson, A.H., Rasmussen, M., Pedersen, O.D, Dønstrup, S., Andersen, H.J. (2001). Origin of multiexponential T2 relaxation in muscle myowater, J. Agric. Food Chem. 49 (6),3092–3100 doi: 10.1021/jf001402t

Bertram, H.C., Andersen, R.H., Andersen, H.J. (2007). Development in myofibrillar water distribution of two pork

qualities during 10-month freezer storage, Meat Sci. 75(1), 128-133, doi: 10.1016/j.meatsci.2006.06.020

Braslavsky, I. (2015) Control of ice formation in biological samples, Cryobio., 71 (1), 168, doi: 10.1016/j.cryobiol.2015.05.021

Butler, J.P, Reeds, J.A., Dawson, S.V., (1981) Estimating Solutions of First Kind Integral Equations with Nonnegative Constraints and Optimal Smoothing, SIAM J. Numer. Anal., 18(3), 381–397, doi: 10.1137/0718025

Callaghan P.T. (1993) Principles of Nuclear Magnetic Resonance Microscopy. Oxford University Press

Carr, H., Purcell, R., (1954) Effects of diffusion on free precession in nuclear magnetic resonance experiments, Phys. Rev., 94,630–638 doi: 10.1103/PhysRev.94.630

Chen, Y.C. and Pan, B.S. (1997) Morphological changes in tilapia muscle following freezing by air-blast and liquid nitrogen methods. Int. J. Food Sci. Tech. 32, 159–168.

Dalvi-Isfahan,M., Jha, P.K, Tavakoli, J., Daraei-Garmakhany , A., Xanthakis , E., Le-Bail, A., (2019). Review on identification, underlying mechanisms and evaluation of freezing damage., J. Food Eng., 255: 50-60, doi: 10.1016/j.jfoodeng.2019.03.011

Delgado A., Sun DW. (2011) Ultrasound-Assisted Freezing. In: Feng H., Barbosa-Canovas G., Weiss J. (eds) Ultrasound Technologies for Food and Bioprocessing. Food Engineering Series. Springer, New York, NY

Duflot, M., Sanchez-Alonso, I., Duflos, G., Careche, M., (2019). LF 1H NMR T2 relaxation rate as affected by water addition, NaCl and pH in fresh, frozen and cooked minced hake., Food Chem, 277: 229-237, doi: 10.1016/j.foodchem.2018.10.106

Duun, A.S., Rustad, T. (2007) Quality changes during superchilled storage of cod (Gadus morhua) fillets

Erikson, U., Veliyulin, E., Singstand, T.E., Aursand, I.G., (2004). Salting and Desalting of Fresh and Frozen-thawed Cod (Gadus morhua) Fillets: A Comparative Study Using 23Na NMR, 23Na MRI, Low-field 1H NMR, and Physicochemical Analytical Methods. J Food Sci, 69(3): 107-114, doi: 10.1111/j.1365-2621.2004.tb13362.x

Fischler, C., (2002). Food selection and risk perception. In: Anderson, H., Blundell, J., Chiva, M. (Eds.), Food Selection: From Genes to Culture. Danone Institute, pp. 135–149.

388 Gudjonsdottir, M., Traore, A., Jonsson, A, , Karlsdottir, M.G., Arason, S. (2015) The effects of pre-salting methods
389 on salt and water distribution of heavily salted cod, as analyzed by 1H and 23Na MRI, 23Na NMR, low-field
390 NMR and physicochemical analysis. Food Chem. 188 (1): 664-672. doi: 10.1016/j.foodchem.2015.05.060

391 Haralick, R. M., Sternberg, S. R., & Zhuang, X. (1987). Image Analysis Using Mathematical Morphology. IEEE
392 Transactions on Pattern Analysis and Machine Intelligence, 4, 532–550, doi: 10.1109/TPAMI.1987.4767941

393 Harzallah, H., Jurie, F., Schmid, C., (2009). Combining efficient object localization and image
394 classification. Proc. IEEE Int. Conf. Comput. Vis. 237–244.
395 https://doi.org/10.1109/ICCV.2009.5459257

396 Howell, N., Shavila, Y., Grootveld, M., Williams, S., (1996). High-Resolution NMR and Magnetic Resonance
397 Imaging (MRI) Studies on Fresh and Frozen Cod (Gadus morhua) and Haddock (Melanogrammus
398 aeglefinus). J Sci. Food Agri., 72(1): 49-56, doi: 10.1002/(SICI)1097-0010(199609)72:1<49::AID-
399 JSFA621>3.0.CO;2-H

400 Hurling, R., McArthur, H., (1996) Thawing, refreezing and frozen storage effects on muscle functionality and
401 sensory attributes of frozen cod (Gadus morhua). J. Food. Sci., 61, 1289-1296. doi: 10.1111/j.1365-
402 2621.1996.tb10981.x

403 Jensen, K.N., Guldager, H.S., Jørgensen, B.M., (2002). Three-Way Modelling of NMR Relaxation Profiles from
404 Thawed Cod Muscle. J Aq. Food Prod. Technol, 69(3): 107-114, doi: 10.1111/j.1365-2621.2004.tb13362.x

405 Johnston, W.A. Nicholson, F.J. Roger, A. Stroud, G.D, (1994) Freezing and refrigerated storage in fisheries, FAO,
406 Rome (Italy). Fisheries Dept.

407 Lambelet, P., Renevey, F., Kaabi, C., Raemy, A. (1995). Low-Field Nuclear Magnetic Resonance Relaxation Study
408 of Stored or Processed cod. J Agr. Food Chem, 43: 1462-1466, doi: 10.1021/jf00054a009

409 Love, R.M. (1956) Influence of Freezing-rate on the Denaturation of Cold-stored Fish, Nature, 178: 988-989, doi:
410 10.1038/178988a0

411 MacCallums, W.A., Laishley, E.J., Dyer, W.J., Idler, D.R. J.P. (1966). Taste panel assment of Cod fillets after single
412 and double freezing. J. Fish. Res. Bd. Canada 23 1063-1081. doi: 10.1139/f66-097

Meiboom, S., Gill, D., (1958) Modified spin-echo method for measuring nuclear relaxation times, Rev. Sci., 29,688, doi: 10.1063/1.1716296

Mortensen, M., Andersen, H.J,Engelsen, S.B., Bertram, H.C. (2006). Effect of freezing temperature, thawing and cooking rate on water distribution in two pork qualities, Meat Sci. 72(1), 34-42, doi: 10.1016/j.meatsci.2005.05.027

Mørkøre, T., Lilleholt, R., (2007). Impact of freezing temperature on quality of farmed Atlantic Cod (Gadus Horhua L.), J. Text. Stud. 34(4), 457-472, doi: 10.1111/j.1745-4603.2007.00108.x

Nakazawa, N., Okazaki, E. (2020) Recent research on factors influencing the quality of frozen seafood, Fish Sci, 86, 231-244 doi: 10.1007/s12562-020-01402-8

Nott, K.P., Evans, S.D., Hall, L.D., (1999). The Effect of Freeze-Thawing on the Magnetic Resonance Imaging Parameters of Cod and Mackerel, LWT Food Sci Tech 32(5): 261-268, doi: 10.1006/fstl.1999.0549

Ofstad, R., B. Egelandsdal, S. Kidman, R. Myklebust, R. L. Olsen, and A. M. Hermansson. (1996). Liquid loss as effected by post mortem ultrastructural changes in fish muscle: Cod (Gadus morhua L) and salmon (Salmo salar). J Sci Food Agr 71(3):301-3123. doi:10.1002/(SICI)1097-0010(199607)71:3

Petzold G., Aguilera J. M., (2009) Ice morphology: Fundamentals and technological applications in foods. Food Biophysics. 4(4):378–396. doi: 10.1007/s11483-009-9136-5

Powrie, W.H. (1984) Chemical Effects during Storage of Frozen Foods, J. Chem. Educ. 61 (4), 340, doi: 10.1021/ed061p340

Russakovsky, O., Deng, J., Su, H., Krause, J., Satheesh, S., Ma, S., Huang, Z., Karpathy, A., Khosla, A., Bernstein, M., & Berg, A. C. (2015). ImageNet Large Scale Visual Recognition Challenge. International Journal of Computer Vision, 211–252, doi: 10.1007/s11263-015-0816-y

Saez, M.I., Suarez, M.D., Cardenas, S., Martinez, (2015) T.F. Freezing and Freezing-Thawing Cycles on Textural and Biochemical Changes of Meagre (Argyrosomus regius, L) Fillets During Further Cold Storage, Int. J. Food Prop, 18 (8), 1635-1647 doi: 10.1080/10942912.2014.919319

Sánchez-Alonso, I., Martinez, I., Sanchez-Valencia, J., Careche, M. (2012) Estimation of freezing storage time and quality changes in hake (Merluccius merluccius, L.) by low field NMR, Food Chem, 135(3), 1626-1634, doi:

10.1016/j.foodchem.2012.06.038

Sánchez-Alonso, I., Moreno, P., Careche, M. (2014) Low field nuclear magnetic resonance (LF-NMR) relaxometry in hake (Merluccius merluccius, L.) muscle after different freezing and storage conditions, Food Chem, 153, 250-257, doi: 10.1016/j.foodchem.2013.12.060

Shibata, Y., Matsumura, A., Meguro, K., Narushima, K. (2000), Differentiation of mechanism and progmosis of traumatic brain stem lesions detected by magnetic resonance imaging in the acute stage, Clin. Neuro. Neurosurgry, 102(3), 124-128 doi: 10.1016/S0303-8467(00)00095-0

Sigurgisdottir, S., Ingvarsdottir, H., Torrissen, O., Cardinal, M., Hafsteinsson, H., (2000) Effects of freezing/thawing on the microstructure and the texture of smoked Atlantic salmon (Salmo salar), Food. Res. Int, 33(10): 857-865, doi: 10.1016/S0963-9969(00)00105-8

Simonyan, K., & Zisserman, A. (2015). Very deep convolutional networks for large-scale image recognition. 3rd International Conference on Learning Representations, ICLR 2015 - Conference Track Proceedings, 1–14, doi: 10.1109/ACPR.2015.7486599

Srivastava, N., Hinton, G., Krizhevsky, A., Sutskever, I., & Salakhutdinov, R. (2014). Dropout: A Simple Way to Prevent Neural Networks from Overfitting. Journal of Machine Learning Research, 15, 1929–1958, doi: 10.5555/2627435.2670313

Stormo, S.K., Skåra, T., Skipnes, D., Sone, I. Carlehog, M., Heia, K., Skjelvareid, M.H., (2018). In-Pack Surface Pasteurization of Capture-Based, Pre-Rigor Filleted Atlantic Cod (Gadus morhua). J Aq. Food Prod. Technol, 27(7): 783-794, doi: /10.1080/10498850.2018.1499161

Szegedy, C., Toshev, A., Erhan, D., 2013. Deep Neural Networks for Object Detection, in: Proceedings of the 26th International Conference on Neural Information Processing Systems. Curran Associates Inc., Red Hook, NY, USA, pp. 2553–2561.

van der Sman, R. G. M., Voda, A., van Dalen, G., & Duijster, A. (2013). Ice crystal interspacing in frozen foods. Journal of Food Engineering, 116(2), 622-626, doi: 10.1016/j.jfoodeng.2012.12.045

Veliyulin, E., Aursand, I.G., (2007). 1H and 23Na MRI studies of Atlantic salmon (Salmo salar) and Atlantic cod (Gadus morhua) fillet pieces salted in different brine concentrations J Sci. Food Agri., 87(14): 2676-2683,

465 doi: 10.1002/jsfa.3030

466 Washburn, K.E., Stormo, S.K, Skjelvareid, M.H., Heia, K., (2017). Non-invasive assessment of packaged cod freeze-
467 thaw history by hyperspectral imaging. J Food Eng., 205: 64-73, doi: 10.1016/j.jfoodeng.2017.02.025

468 Welch, K.M.A, Windham, J., Knight, R.A., Nagesh, V., Hugg, J.W., Jacons, M., Peck, D., Booker, P., Dereski, M.O.,
469 Levine, S.R. (1995) A Model to predict the histopathology of human stroke using diffusion and T2-weighted
470 magnetic resonance imaging, Stroke, 26(11), 1983-1989, doi: 10.1161/01.STR.26.11.1983

471 Xu, J.L., Sun, D.W (2017). Identification of freezer burn on frozen salmon surface using hyperspectral imaging and
472 computer vision combined with machine learning algorithm. Int. J Refridg.74: 151-164, doi:
473 10.1016/j.ijrefrig.2016.10.014

474 Yushkevich, P.A., Piven, J., Hazlett, H.C., Smith, R.G., Ho, S., Gee, J.C., Gerig, G., 2006. User-guided 3D active
475 contour segmentation of anatomical structures: Significantly improved efficiency and reliability.
476 Neuroimage 31, 1116–1128. https://doi.org/10.1016/j.neuroimage.2006.01.015